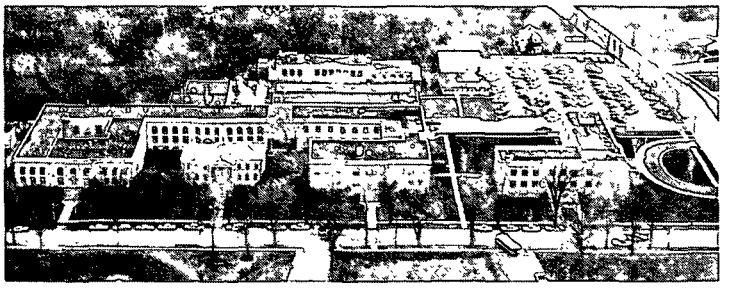

THE INSTITUTE OF PAPER CHEMISTRY, APPLETON, WISCONSIN

IPC TECHNICAL PAPER SERIES
NUMBER 243

BLACK LIQUOR COMBUSTION IN A LABORATORY FLOW REACTOR — STATUS REPORT ONE

D. T. CLAY AND H. G. SEMERJIAN

JUNE, 1987

Black Liquor Combustion in a Laboratory Flow Reactor - Status Report One

D. T. Clay and H. G. Semerjian

This manuscript is based on results obtained in IPC Project 3473-6 and is to be presented at the TAPPI Engineering Conference in New Orleans on September 13-17, 1987

BLACK LIQUOR COMBUSTION IN A LABORATORY FLOW REACTOR - STATUS REPORT ONE

D. T. Clay,
Associate Professor
The Institute of
Paper Chemistry
P.O. Box 1039
Appleton, WI 54912

H. G. Semerjian
Group Leader
A. Macek
Research Chemist
National Bureau of Standards
Gaithersburg,MD, 20899

ABSTRACT

The Office of Industrial Programs, U.S. Department of Energy, funds a 5-year research effort at IPC and NBS to study fundamentals of kraft black liquor combustion. Two complementary flow reactor systems, one for process and the other for dilute-phase studies, are now in place. Mill kraft black liquor droplets, nominally 2 mm at up to 68% solids, are continuously fed into simulated furnace environments. These systems have been used to study early in-flight process dynamics, char formation processes, and the physical and chemical characteristics of char and its precursors. This paper discusses significant results to date and summarizes the project's future direction.

INTRODUCTION

The efficient recovery of chemicals and high level energy from black liquor contributes heavily toward the dominance of the kraft pulping process. Kraft pulp represents 74% of North American market pulps (1). Kraft recovery boilers used to burn black liquor have been commercially available for over 50 years. Since the basic process knowledge is only now being developed, the potential exists for significant improvements in energy recovery and black liquor throughput (2,3).

A relatively conservative estimate of the potential improvements results in energy savings of 5×10^5 Btu/adtp and an incremental production increase of 1%. These are equivalent to nominally $200,000,000/yr for the industry (4). Advances to achieve these and hopefully higher benefits can only be done with a fundamental knowledge of the controlling combustion phenomena. Once the controlling phenomena are identified, recovery boilers can be pushed to their ultimate acceptable limits. In practice, the results will also be a starting point for design of equipment, e.g., improved liquor and air delivery systems, to reach and hopefully raise these limits.

The importance of process fundamentals was identified in the American Paper Institute sponsored work of Merriam (5). Two books (6,7) also identify this need. Recent advances have been made to understand kraft black liquor combustion with molten salt and single particle studies (8-13). Four stages of black liquor burning are identified: drying, volatiles burning, char burning, and smelt coalescence. Additional understanding in each one of these stages is needed for application to continuous flowing systems. The increased knowledge should provide a bridge for application of prior or new results to commercial recovery boilers.

The Office of Industrial Programs, U.S. Department of Energy, and The Institute of Paper Chemistry sponsor a project to obtain fundamental data on black liquor combustion. The project began in October 1983 and extends for five years. The three objectives of the project focus on advancing kraft recovery boiler process understanding:

a) Develop continuous flow systems to study both state-of-the-art and advanced recovery processes.
b) Apply advanced optical and spectroscopic techniques to study the burning processes.
c) Develop a data base of process fundamentals which will bridge and enhance the commercial application of prior and new research findings.

These objectives will be accomplished in four phases. These are:

Phase 1. In-flight chemical and thermal processes
Phase 2. Char bed processes
Phase 3. Inorganic fume formation processes
Phase 4. Recovery furnace simulation

Two continuous laboratory scale systems, one at The Institute of Paper Chemistry (IPC) and one at the National Bureau of Standards (NBS), provide the equipment to study the burning processes. The IPC system is used for overall process studies and complete furnace simulation. The NBS dilute-phase system is for instrumentation development and single particle tests.

The work to date has focused on Phase 1, in-flight chemical and thermal processes. The emerging view is that initial liquor characteristics, specifically the droplet size, viscosity and swelling tendency, are major variables affecting both the initial burning processes and particle trajectory. Projects which seek to increase recovery boiler performance need to address these critical issues. This paper will discuss results that lead to this conclusion, the two experimental systems, and future direction of the project.

EXPERIMENTAL

IPC Flow Reactor

Process studies which emphasize the chemical composition of solid, liquid, and/or gaseous products are the focus of the IPC Process Flow Reactor System. Figure 1 shows a schematic of the flow reactor system. Electrical preheaters bring the air, nitrogen, or a mixture of the two to the desired temperature before entry into the reactor base.

The inner fused alumina lining is nominally 4-inch (100 mm) I.D. The entire nominal 14 ft (4.3 m) length of the in-flight section is encased with cylindrical electrical heaters. The gas temperature stays approximately constant over this length. The first and second progress reports to DOE list the system details (4,14).

The Phase 1 system provides for continuous feeding of black liquor droplets at realistic droplet injection temperatures. In this configuration, continuous operation can be achieved within four hours.

1

All tests covered in this paper were in the gas upflow mode. Table 1 lists nominal test conditions for the results discussed below. Actual operating ranges are wider.

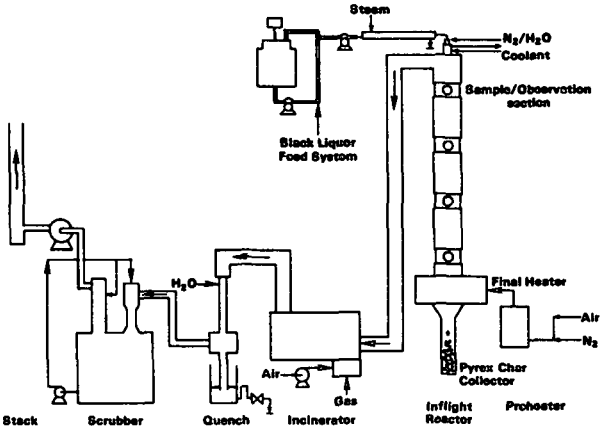

Fig. 1. Upflow mode of IPC Phase 1 system.

Table 1. Test group 1 nominal conditions for the IPC reactor system.

Black Liquor Feed	Flow	1.3 lb solids/h (15 g liquor/min)
	Temperature	200 to 240°F (93 to 115°C)
	Solids	65%
	Droplet size	nominally 2mm
Gas Characteristics	Flow rate	4 scfm (113 std. Lpm)
	Velocity	3 ft/sec (1 m/sec)
	Temperature	1615°F (880°C)
	Oxygen	0 to 21%
Longest Sustained Operating Period	6 hours with liquor feed 10 hours including times without liquor feeding	

NBS Short-Height DPFR

Measurement of size and velocity on free-falling single droplets/particles has been the initial diagnostic work with the short-height dilute-phase flow reactor (DPFR) at NBS. Figure 2 shows a schematic representation of the system. The vertically positioned quartz tube is 4-inch I.D. The system construction details have previously been listed (4).

Hot gases, having the desired temperature and free-oxygen concentration are admitted through the bottom section. Combustion products of a premixed propane/air flame are diluted with the required amount of air or nitrogen. Black liquor droplets form on the tip of the injector at the top of the reactor. The nominal length of droplet fall is 30 inches (760 mm). Since the quartz section is not insulated there is a nominal temperature gradient from top to bottom of 20°F/inch (440°C/m).

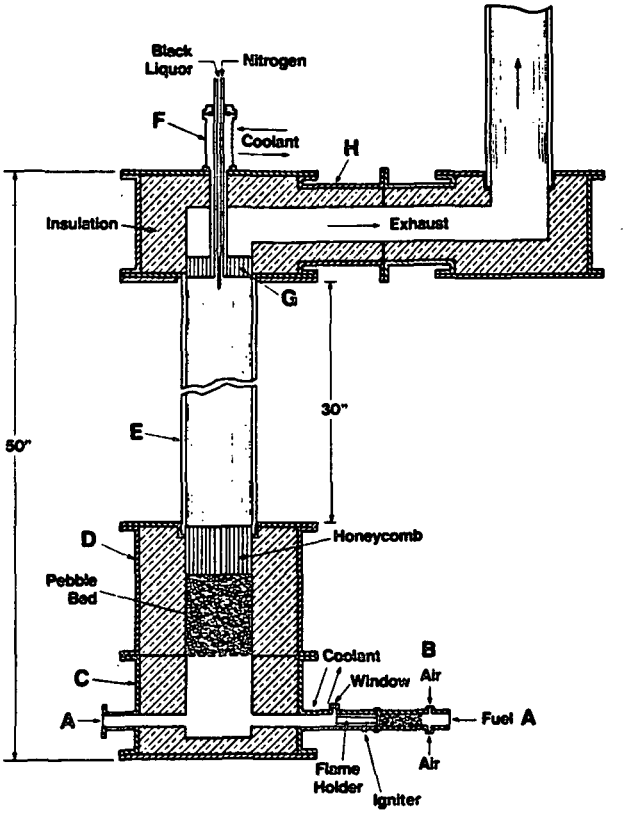

Fig. 2. Dilute phase flow reactor (short-height). A. Dilution air inlet. B. Gas burner. C. Mixing Chamber. D. Flow straightener. E. Quartz tube. F. Droplet injector. G. Flow straightener. H. Exit section.

The operating conditions used in the tests to be discussed below are shown in Table 2.

Table 2. Nominal test conditions for the NBS short-height DPFR.

Black Liquor Feed	Flow	one drop at a time
	Temperature	nominal 195°F (90°C)
	Solids	65%
	Droplet size	nominally 2mm
Gas Characteristics	Flow rate	7 to 16 scfm (200 to 450 std. Lpm)
	Velocities	5 to 14 ft/sec (1.5 to 4.3 m/sec)
	Temperatures	2100 to 1340°F (1150 to 725°C)
	Oxygen	1.5 to 21%

Black Liquor

The black liquor samples used for all the tests reported in this paper came from a north central kraft mill. Normal mill furnish is 57% hardwood and 43% softwood. Continuous digestors are used to cook to a kappa number of 16. Liquor oxidation is practiced at this mill. Samples were collected after the evaporators and after the mix tank near

2

the recovery boiler. The analysis will be presented in Table 4.

IPC PROCESS STUDIES

Preliminary tests suggested that particle residence times were nominally 1.5 seconds. This is sufficient time to essentially complete drying and initiate the char forming processes. The dynamic increase in specific swollen volume was the major reason for longer residence times than those previously anticipated (4). The influence of upward flowing N_2 was minimal. The early in-flight processes appear dominated by heat transfer to the particle as it dries and pyrolyzes. Virtually all particles impacted the wall. Most bounced off after a short contact time with the wall. The extent of wall impact and subsequent retention depended upon conditions. When the air flow was 4 scfm (113 std. Lpm) or less and the temperature was above 1525°F (830°C) the majority of particles hit but did not stick on the walls.

Approach

The systematic study of the in-flight processes began by studying the influence of six process variables on the chemical and physical characteristics of the produced chars. Three test groups were planned to study two variables each. The variables and their groups were gas phase O_2 content and liquor temperature, gas flow rate and temperature, particle size and liquor solids content. This paper summarizes the results of the first test group.

The objective of test group 1 was to evaluate the effect of gas phase O_2 content and black liquor injection temperature on the chemical and physical properties of the produced chars. A complete factorial with three levels for each variable plus two replicates was planned.

The base operating conditions for the reactor were listed in Table 1. The level for the two variables plus the variation in liquor solids is listed in Table 3.

Table 3. Group 1 test independent variable levels.

Test	Oxygen, % volume	Temperature of Liquor (°F)	(°C)	Feed Solids, % ODS
47	0	199	93	67.4
50	0	207	97	64.8
51	21	200	94	64.8
52	0	215	102	64.0
53	21	217	103	64.0
54	21	217	103	64.0
56	10	221	105	64.0
57	10	239	115	64.0
58	10	203	95	64.0
59	21	219	104	64.0
60	21	241	116	63.6

ODS - Oven dried at 221°F (105°C).

The O_2 level was set by either using N_2, air, or a quantitative blend of the two. The average O_2 level for the 10% and 21% inlet cases was slightly less due to partial combustion. There was some air infiltration due to the slight negative pressure in the reactor and hence, at the 0% O_2 level, some O_2 probably existed. The liquor temperature is the exit injector coolant temperature adjacent to the black liquor feed. The solids variations occurred because of slight water leaks into the liquor supply between tests.

Results

The average and range of the chemical and physical char characteristics produced in the IPC process tests are listed in Table 4. The properties of the initial liquor are also listed for comparison.

Table 4. Average physical and chemical properties of test group 1 product chars.

	Feed Liquor No. 41A	Product Char Average ± 95% CL*	Range
Fixed carbon, % ODS**	0	4.42 ± 1.41	2.65-10.27
Moisture, % ODS	64.4 ± 0.7	1.53 ± 0.45	0.55-2.71
Swollen volume, cc/g-solid	Approx. 1.2	9.8 ± 2.2	4.2-16
Bulk density, g/L	1300	83 ± 17	27-113
Elements (All values, % ODS)			
C	35.7	31.3 ± 1	27.4-33.0
H	3.25	2.59 ± 0.22	1.85-3.10
O	34.3	35.5 ± 0.4	34.5-36.4
S	4.56	4.5 ± 0.3	3.8-5.2
Na	19.8	22.3 ± 0.8	20.2-24.6
K	1.4	2.93 ± 0.12	2.74-3.28
Material balance, %	99	98.5 ± 0.8	96.8-100
Na_2CO_3	7.97	27.8 ± 3.3	22.8-38.0
Na_2SO_4	5.87	8.08 ± 1.11	6.71-11.7
Na_2SO_3	0.96	1.66 ± 0.38	1.01-2.80
$Na_2S_2O_3$	8.19	4.64 ± 0.54	3.27-5.71
Na_2S	0	0.85 ± 0.41	0.14-2.15

*CL - confidence limits.
**ODS - oven dried solids at 221°F (105°C).

Comparison of these data with equilibrium pyrolysis of single particles of the same liquor show that the char is only partially pyrolyzed. It is also interesting to note that moisture still remains in the char even though pyrolysis has begun. This is a good indication that particle temperature gradients exist and that there is overlapping of the burning stages.

Despite the fact that pyrolysis was only partially complete, substantial sustained swelling occurred. The swollen volume increased on average over 8 times and the char bulk density decreased over 15 times. The factors controlling the swelling process (10,11) appear to be mainly operable during the latter phases of drying and the early phases of pyrolysis.

Most of the chemical shifts were as expected. Table 5 lists the percent change of the major components. Based on the change in Na the average solids mass loss was 11%. The major elements lost were C, H, O, and S.

3

Table 5. Average percent change in chemical components during char forming processes of test group.

	Average ± 95% CL*	Range
Carbon loss, %	22.2 ± 4.9	9.3-33.8
Hydrogen loss, %	33.2 ± 7.6	12.6-46.5
Oxygen loss, %	11.2 ± 3.3	2.0-20.5
Sulfur loss, %	11.9 ± 6.3	0.1-32.8
$Na_2S_2O_3$ loss, %	49.2 ± 7.2	34.6-67.9
Na_2CO_3 gain, %	208 ± 27	170-288
Na_2SO_4 gain, %	23.2 ± 14.7	-1.7-71.9
Na_2SO_3 gain, %	52.7 ± 32	3.1-151
S=/S, %	7.7 ± 3.7	1.5-20.0
FC/C, %	12.7 ± 4.4	7.2-31.7

*CL - confidence limits.

It is interesting to note that there is on average a higher carbon loss than sulfur loss. The tested liquor is an oxidized liquor. A substantial percentage (70%) of the sulfur is as $Na_2S_2O_3$. Sodium thiosulfate showed a 50% loss during these tests. It decomposes rapidly at relatively low temperatures. Literature data (15) support decomposition to Na_2SO_4, Na_2S, and elemental sulfur at temperatures from 433 to 878°F (225 to 470°C). The present data support the reaction products. Note that Na_2S was in the product char. In the cooler regions of the reactor, yellow deposits presumed to be sulfur were found during an inspection following these tests.

The low mass loss, sulfur loss, fixed carbon values, and visual observations support the hypothesis that only relatively low particle temperatures were achieved. Sulfide formation and elemental sulfur release via $Na_2S_2O_3$ decomposition is one of the early in-flight sulfur release processes in the particles.

During these 11 tests the feed solids changed from 67.4 to 63.6%. Feed solids content effectively became a third independent variable. Unfortunately, the unplanned variation in feed solids had a significant trend with liquor temperature. Higher feed solids were present when higher liquor temperatures were tested. This trend makes it difficult to separate the two variables.

Significant effects of the three independent variables on char characteristics were identified with Student's t-test (16). Single and multiple dependencies were tested. The relationships which were significant at the 95% level (t-values > 2.2) are listed in Table 6. Larger t-values imply a higher degree of significance.

The listed t-values are for the single independent variables' relationship with the char characteristic. No multiple relationships were significant.

Table 6. Char characteristics which had a significant relationship with one of the three independent variables.

Char Characteristic	Indep. Variable	t-value*
Swollen volume	Liquor temperature	+2.3
	Feed liquor solids	-2.4
Swollen volume confidence limits	Liquor temperature	+2.7
	Feed liquor solids	-2.9
C/Na_2 percent loss	Liquor temperature	+2.2
CO_3/Na_2 percent gain	Gas phase O_2 level	-2.2
SO_4/Na_2 percent gain	Feed liquor solids	+4.5
SO_3/Na_2 percent gain	Feed liquor solids	+4.2
	Liquor temperature	-2.6
S_2O_3/S percent in char	Liquor temperature	+2.2

*Based on Student's t distribution.

Increased liquor temperature produced larger and more variable swollen volumes, greater carbon loss, less Na_2SO_3 in the char and a higher percentage of the char S as $Na_2S_2O_3$.

Lower liquor solids produced higher and more variable swollen volumes, and less Na_2SO_4 and Na_2SO_3 in the char. As noted above, variations caused by feed solids and liquor temperature may not be completely separable. Fortuitously, the direction of both consistently changes the liquor viscosity, so that at least cancelling effects should not be present.

Lower O_2 levels produced higher Na_2CO_3 levels in the char. It should be noted that the other char analyses had no significant relationship with the three variables.

The changing environment that the particle encounters in the reactor produces significant dynamic changes in its physical as well as its chemical character. The initial results of NBS document these changes.

NBS SINGLE PARTICLE STUDIES

Approach

In-flight studies of black liquor droplets/particles were done with a high-speed camera, 500 frames per second. The field viewed by the camera was 3.9 inches (100 mm) horizontal by 3.2 inches (80 mm) vertical. Three sets of determinations were made at three locations in the short-height DPFR; top, center, and near the bottom. The initial droplet diameter was determined via a permanently mounted video camera.

To obtain in-flight droplet diameter and velocity a standard reference length is filmed, along

4

with the droplets, from which a magnification factor is calculated. The droplet velocity is obtained by counting the number of frames of film used by the particle to move over a certain known distance.

Droplet/particle velocity calculations were also made. A computer program calculates particle velocities and distances from the injection point by balancing the gravitational force against buoyant and drag forces due to upward gas flow. Since the calculated velocities are very weak functions of temperature, all calculations were made for gas temperatures of 1560°F (850°C) with virtually no sacrifice of accuracy.

Results

Top of DPFR

The main purpose of high-speed photography, in this section of the reactor, was (a) to observe the process of detachment from the needle and initial trajectories of black liquor droplets, and (b) to measure their velocities. The top of the DPFR is defined as the first 2.8 inches (70 mm) below the injection point.

The process of black liquor droplet detachment from the needle is abrupt. No lingering droplet tails formed. This is advantageous, because it decreases the chances of droplet drying and distortion before detachment. The droplets became spherical immediately after detachment. Finally, the initial droplet trajectories were vertical.

The droplet started at zero velocity and showed rapid acceleration over the viewed segment. The experimental velocities given in Table 7 are the final values before the disappearance of the droplet from the field of view.

Table 7. Velocities at the top of DPFR.

d, mm	U_g	U_p (exp)	U_s (exp)	U_s (calc)	U_t (calc)
1.7	4.36 (1.33)	4.00 (1.22)	8.36 (2.55)	7.93 (2.42)	29.2 (8.91)
2.1	5.15 (1.57)	3.54 (1.08)	8.69 (2.65)	8.75 (2.67)	36.1 (11.00)

Velocity Units, ft/sec (m/sec).
exp = experimental calc = calculated.

U_g - upward gas velocity from measured volumetric rates and local temperature.
U_p - particle velocity relative to laboratory coordinates.
U_s - particle velocity relative to gas (slip velocity).
U_t = particle terminal velocity relative to gas.

The agreement between the experimental and calculated U_s values is good. Table 7 also gives the computed terminal (settling) velocity, U_t, which U_s would approach at long times if the droplet remained physically unchanged. The droplets are still accelerating in the top of the DPFR. Another aspect of the experimental and calculated results in the top of DPFR is that they give a good definition of initial conditions. The nominal residence time from injection to leaving this field of view was 0.10 second.

Center of DPFR

The camera was centered at 16 inches (400 mm) below the injector. At this height there is not one-to-one correspondence between the droplets at injection and droplet/particles measured by high-speed films. The procedure adopted in these studies was to relate the properties of droplets/particles observed by high-speed photography (shapes, sizes, and velocities) to average initial diameters from VCR measurements. Most falling particles were still nearly spherical and were almost always falling vertically near the center of the reactor. Moderate expansion of particles was observed. This implies density decreases. In addition, there may or may not have been mass losses due to vaporization.

Table 8 gives the data for four individual particles at a fixed set of test conditions. The format is similar to that in Table 7, with two differences. First, the ratio d/d_o is given, because it is a parameter necessary for calculation of velocities. The second difference, also due to the lack of continuous recording, is that the calculation of U_s is not straightforward, but requires some assumptions, as discussed below.

Table 8. Velocities at the center of the DPFR.

		Experimental		Calculation A		Calculation B	
	d/do	U_p	U_s	U_s	U_t	U_s	U_t
	1.6	6.92 (2.11)	16.9 (5.16)	15.0 (4.57)	16.8 (5.11)	12.7 (3.88)	12.4 (3.79)
	1.4	7.25 (2.21)	17.2 (5.26)	15.7 (4.78)	19.0 (5.81)	14.1 (4.31)	14.1 (4.31)
	1.6	6.92 (2.11)	16.9 (5.16)	15.0 (4.57)	16.8 (5.11)	12.7 (3.88)	12.4 (3.79)
	1.6	7.25 (2.21)	17.2 (5.26)	15.0 (4.57)	16.8 (5.11)	12.7 (3.88)	12.4 (3.79)
Average:	1.55	7.02 (2.14)	17.1 (5.21)	15.1 (4.62)	17.3 (5.28)		12.8 (3.92)

Velocity units = ft/sec (m/sec).

Calculation A - no drying assumed.
Calculation B - complete drying assumed.
Conditions: d_o = 1.6 mm, U_g = 10.0 ft/sec (3.05 m/sec).

Analysis of high speed films yields two experimental quantities: the particle diameter d and the particle velocity U_d, relative to laboratory coordinates. The latter is then converted to the experimental slip velocity U_s (exp) by means of the known upward gas velocity U_g. While all three measurements - d, U_p, and U_g - are subject to experimental errors, their determination does not require the knowledge of the initial diameter d_o. It is important to note that the calculations of terminal velocities, U_t, are also independent of

5

d_o, being determined only by the particular diameter which is measured, and the particle density which must be assumed. Therefore, for the purpose of data analysis, it was useful to calculate two sets of U_t values with different particle densities: one for no mass loss from the original droplets (assumption A) and the other for complete drying, i.e., 35% mass loss (assumption B).

The experimental and calculated velocities are given in Table 8. Inspection of the columns which are based only on measurements of expanded particles (i.e., independent of numerical values of d_o), show good agreement between the experimental U_s and the U_t calculated on the assumption of no drying. This shows that the assumption of any degree of drying would give two low values of calculated U_s and U_t. Thus the data are consistent with the concept of expanded particles, with little or no mass loss, settling against the upward gas flow.

In contrast to the experimental U_s and the calculated U_t values, the calculated U_s values depend not only on the extent of mass loss, but also (a) on the value of d_o and (b) on assumptions regarding the expansion history of the droplets. A reasonable choice regarding the expansion history was to break up the calculation of the two parts: one up to 2.8 inches (70 mm) of travel with the initial droplet diameters and densities, and the second with final particle diameters d. As in the case of U_t calculations, two sets of U_s values were obtained (assumptions A and B). A comparison of these with the experimental U_s, again, shows that the assumption of drying is not at all reasonable. In fact, it can be seen that even the assumption of no drying yields calculated U_s values at or about 13% low. This difference can probably be ascribed to the uncertainties in calculation assumptions and to experimental errors.

Bottom of DPFR

The most extensive set of data was obtained in the bottom of the DPFR, centered at 29 inches (740 mm) below the point of droplet injection. The data were taken in a series of 14 runs, each lasting about 10 seconds, during which period about 30 to 50 black liquor droplets were released from the injector.

The analysis of high-speed records revealed that most of the falling particles were again nearly spherical. Table 9 lists the average values of the initial droplet diameters, d_o, in each of fourteen runs, and the corresponding average values, d, of particles at the bottom.

Each of these average values is the arithmetic mean of at least ten individual readings. Table 9 shows that the average linear expansion, d/d_o, is about 1.5. There is substantial scatter. The tested levels of oxygen concentration had no noticeable effect. Another effect which may be expected is that smaller initial droplet diameters should have a longer residence time between injection and observation. This is not apparent from the data.

Table 9. Initial black liquor diameter, and expanded diameter at the bottom of the DPFR.

O_2 in Gas, %	Initial Dia d_o, mm	Expanded Dia d, mm	Ratio, d/d_o
1.5	1.7	2.6	1.5
2.2	1.6	2.1	1.3
5.1	1.7	2.5	1.5
8.4	1.7	2.4	1.4
9.4	1.3	2.2	1.1
9.5	1.7	2.2	1.3
9.7	1.6	2.5	1.6
9.8	1.6	2.7	1.7
9.8	1.7	2.7	1.6
10.1	1.5	2.1	1.4
10.3	1.6	2.9	1.8
16.7	1.4	2.4	1.7
16.9	1.6	2.0	1.3
20.9	2.0	3.1	1.6

Gas Conditions: upflow at 8.3-12.8 ft/sec (2.5-3.9 m/sec) 1740°F (950°C)

The velocity results are shown in Table 10 in the same format as Table 8. This table also includes a calculated estimate of the residence time. The experimental U_s and calculated U_t are based only on direct velocity and diameter measurements, while the calculated U_s and t_R were determined in two stages.

Table 10. Droplet velocities and residence times near bottom of DPFR.

Experimental			Calculation A			Calculation B		
d_o, mm	d/d_o	U_s	U_s	U_t	t_R, sec	U_s	U_t	t_R, sec
1.62[a]	1.52[a]	19.4[a] (5.91[a])	16.6 (5.07)	18.4 (5.60)	0.56	13.7 (4.19)	13.8 (4.20)	0.66
1.7	1.5	17 (5.1)	16 (4.8)	19 (5.9)	0.49	13 (4.1)	14 (4.4)	0.57
1.6	1.3	17 (5.3)	17 (5.1)	21 (6.5)	0.49	15 (4.5)	16 (4.8)	0.57
2.0	1.6	20 (6.0)	18 (5.4)	21 (6.4)	0.51	15 (4.6)	16 (4.8)	0.61
1.7	1.6	20 (6.1)	17 (5.2)	18 (5.6)	0.62	14 (4.2)	14 (4.2)	1.05
1.4	1.7	19 (5.8)	14 (4.3)	14 (4.3)	0.82	11 (3.4)	11 (3.4)	>5

[a]Average of 14 experimental tests shown in Table 9.

t_R = particle residence time estimate from injection until it leaves the bottom field of view.
U_g = 10 ft/sec (3.06 m/sec).
Velocity units ft/sec (m/sec).

The height in the reactor at which droplet expansion begins is unknown. The transition between the two stages is assumed to take place 2.8 inches (71 mm) below the injector. The position assumed does not have a major effect on the calculated velocities or residence times.

6

Table 10 consists of two parts. The first line is based on an overall average of experimental data of 14 runs, listed in Table 9. These original data show initial diameter variations from 1.3 to 1.8 mm and final diameter variations from 2.0 to 3.1 mm. The average gas velocity was U_g = 3.06 m/sec. The second part of Table 10 gives the results of several individual runs.

Inspection of the first line (experimental averages) appears to show a contradiction: even on the assumption of no drying (calculation A), the calculated U_t is lower than the observed U_s. These results illustrate the problem of measurement accuracy. For example, if the measured d/d_o were 6% lower (i.e., if the measured value of d were 2.32 rather than 2.46 mm), U_t would exceed the measured U_s, removing the contradiction. The same would be true, of course, if the measured U_s were 6% lower. Experimental errors of this magnitude are to be expected. On the other hand, experimental errors of 40% would have to be postulated to bring calculation B into agreement with the experiment. The reasonable conclusion, therefore, is that even at the bottom of the DPFR, little mass loss occurred from the particles.

Inspection of results from individual runs in Table 10 provides further illustration of the correctness of the main conclusion: limited drying, if any, after 0.6 second residence in the reactor. On the basis of no drying (calculation A), terminal velocities are seen to exceed U_s, providing the initial diameters are not too small and the measured expanded diameters not too large (expansion ratios not exceeding 1.5 or 1.6). Large expansion ratios, especially when combined with small d_o values, lead to results which can be explained only by invoking inadequate measurement accuracy. The fault, most likely, is with the assignment of d_o which, even for a single line in Table 10, is a calculated average of several individual particles.

Other Observations

The high-speed films show upward moving particles at all locations in the DPFR. Most of these particles had reached the bottom of the reactor, where they either ignited or shattered (or both). In either case they have the potential to be entrained either because of increased diameter or decreased density. The upward moving particles usually had irregular shapes and moved in random trajectories, sometimes hitting the reactor walls and sticking to them. They also had widely different velocities. A few particles had gas flames on top; they were in the volatiles burning stage. In addition, a very few particles were seen to enter the view at low downward velocities, decelerating further, igniting, and reversing their direction of motion (upward). Since average droplets reached the bottom of the short-height DPFR before ignition, it is concluded that these isolated observations of particle ignition were abnormally small.

CONCLUSIONS

Flow reactor systems to study the burning phenomena of kraft black liquor are successfully operating at IPC and NBS. Initial studies have focused on in-flight drying and the early phases of the volatiles burning stage. Overlap between these two stages exists for the nominal 2 mm size particle tested; residual moisture was present even though pyrolysis was well underway.

Both the drying stage and the volatiles burning stage are characterized by droplet/particle swelling. Particle velocity, trajectory, and heat flux to the particle are influenced by swelling. Swelling in the drying stage consists of rapid swelling, bursting, and collapsing. Initiation of swelling comes before significant mass loss. The swelling in the volatiles burning stage continually increases.

Initiation of the volatiles burning stage results in losses of carbon, hydrogen, oxygen, and sulfur. Transitions in the nonvolatile sulfur species also occur in the early phases. Formation of Na_2S was noted despite implied low particle temperatures. Higher feed temperatures and lower feed solids (i.e., lower droplet viscosities) increased the extent of particle reaction. There is minimal effect of the gas-phase oxygen content during these first burning stages.

The data collected to date support the premise that external heat transfer to the particle and the initial liquor conditions, e.g., droplet mass and liquor viscosity, have the greatest influence on the initial burning stages of drying and volatiles burning. The practical significance of this premise is that heat release, black liquor viscosity and spray size need to be controllable parameters for optimum recovery boiler performance.

FUTURE DIRECTION

The in-flight processes studies will continue at both IPC and NBS with emphasis on intermediate sampling at IPC and longer flight times at NBS. Smaller initial droplet sizes will also be tested at IPC with the flow reactor in the gas downflow mode. A two-color pyrometer developed by NBS will be used to measure the particle surface temperature during the burning processes.

The Phase 2 char burning studies will involve construction of a bed burning furnace to replace the Pyrex char catcher on the IPC system. The configuration will allow either batch char bed burning or steady-state bed burning studies.

Phases 3 and 4 will complete this project with work on fume formation and an experimental simulation of simultaneous recovery furnace processes.

ACKNOWLEDGEMENTS

The authors want to thank The U.S. Department of Energy, Office of Industrial Programs, especially program manager Mr. Stanley F. Sobczynski, for support and guidance of this project. The Institute of Paper Chemistry and its member companies also contributed to this project. The support staffs at IPC and NBS, especially Orlin Kuehl, Steve Lien, and N. Amin are responsible for much of the experimental systems and their operation.

LITERATURE CITED

1. Mies, W. E., Allen, D. R., Pollitzer, S., Adams, D., and Espe, C., Pulp and Paper '84, '85 North American Fact Book, Miller Freeman Publications, San Francisco, CA, 1985:237.

2. Grace, T. M., Improved energy efficiency, safety likely in future recovery systems, Pulp Paper, p. 90, October (1981).

3. Grace, T. M., Increasing recovery boiler throughput, Tappi J., **67**(11): 52(1984).

4. Clay, D. T., et. al., Fundamental Studies of Black Liquor Combustion Report No.1 - Phase 1 (October 1983-September 1984), U.S. Department of Eneregy Report DOE/CE/40637-T1 January (1985).

5. Merriam, R. L., Simulation analysis of liquor-firing and combustion processes in kraft recovery furnaces, Tappi J., p. 112, September (1982).

6. Blackwell, B., King, T. K., Chemical Reactions in Kraft Recovery Boilers, Sandwell & Company Ltd. (1985).

7. Hough, G., ed., Chemical Recovery in the Alkaline Pulping Processes, TAPPI Press (1985).

8. Grace, T. M., Cameron, J. H., Clay, D. T., Role of the sulfate-sulfide cycle in char burning: experimental results and implications, Tappi J., p. 108, October (1986).

9. Cameron, J. H., Clay, D. T., Grace, T. M., Oxidative fuming - the phenomenon and possible interpretations, 1985 International Chemical Recovery Conference Preprints, Book 3, p. 435 (1985).

10. Miller, P. T., Clay, D. T., Swelling of kraft black liquor during pyrolysis. Applications of Chemical Engineering Principles in the Forest Products and Related Industries, Volume 1, p. 152, (1986).

11. Miller, P. T., Clay, D. T., Lonsky, W. F. W., The influence of composition on the swelling of kraft black liquor during pyrolysis, TAPPI Engineering Conference Preprints, Book 1, p. 225 (1986).

12. Cantrell, J. G., Sulfur gas release during black liquor burning, M.S. Thesis, Georgia Institute of Technology School of Chemical Engineering, March (1986).

13. Hupa, M., Solin, P., Hyoty, P., Combustion behaviour of black liquor droplets, 1985 International Chemical Recovery Conference Preprints, Book 3, p. 335 (1985).

14. Clay, D. T., et. al., Fundamental Studies of Black Liquor Combustion Report No. 2 - Phase 1 (October 1984-December 1986), U.S. Department of Energy Report DOE/CE/40637-T2 In press (1987).

15. Kubelka, V., Jr., Votoupal, J., Chemical recovery in kraft pulp mills. The chemistry of the recovery process and the design of the recovery unit, Sbornik Vyzkum. Praci z Oboru Celulozy a Papiru 2: 49-73(1957).

16. Hogg, R. V., Craig, A. T., Introduction to Mathematical Statistics, The Macmillan Company, New York (1969).

8